Automated PAM fluorometry as a tool to evaluate the photosynthetic response of *Undaria pinnatifida* to experimental warming

Mary Asumamba Afening

School of Science

2025

A thesis submitted to Auckland University of Technology

in fulfilment of the requirements for the degree of Master of Science (Research)

Supervised by Associate Professor Kay Vopel

Table of content

Attestation of authorship

I hereby declare that this submission is my own work and that, to the best of my knowledge and belief, it contains no material previously published or written by another person (except where explicitly defined in the acknowledgements), nor material that, to a substantial extent, has been submitted for the award of any other degree or diploma from a university or institute of higher learning

Mary Asumamba Afening

Acknowledgements

I would like to express my deepest gratitude to my supervisor, Prof. Kay Vopel, for his invaluable guidance, constructive feedback, and unwavering support throughout the course of this research. Your expertise, patience, and encouragement have been instrumental in shaping both this work and my personal growth as a researcher.

I am sincerely thankful to the Marie Sklodowska–Curie Fellowship of the International Atomic Energy Agency for providing the financial support that made this study possible. Their investment in my education and research is deeply appreciated.

To my family especially my mom and siblings, I am forever grateful for your unconditional love, encouragement, and sacrifices. Your belief in me has been my greatest source of strength.

Finally, I acknowledge Ainslee Binkley, our research intern and all those who, in various ways, contributed to the successful completion of this work.

Abstract

Ocean heatwaves are increasing in frequency and intensity, posing threats to coastal ecosystems. One potentially affected group is seaweeds, whose photosynthetic performance may be disrupted by elevated temperatures. Pulse-amplitude modulation (PAM) fluorometry is a non-invasive technique commonly used to assess species' photosynthetic performance. However, its suitability for unattended and automated in situ monitoring of seaweed photosynthesis under heatwave conditions remains untested. To investigate this, three laboratory experiments were conducted using the invasive kelp species *Undaria pinnatifida*.

In each experiment, one blade from each of three specimens (Experiment 1) or six specimens (Experiments 2 and 3) of *U. pinnatifida*, acclimated in the laboratory under constant temperature and a diel light cycle, was mounted in front of a PAM fluorometer. The blades were held in fixed positions while the fluorometers automatically conducted saturation pulse (SP) analyses at 30-minute intervals—initially during an acclimation period, and subsequently throughout a warming phase. The measuring lights of the PAM fluorometer remained off between analyses, although the blades remained in place for at least 10 days.

SP analyses conducted during the first five hours after light onset each day were used to plot the relative electron transport rate (rETR) and photosynthetically active radiation(PAR) curves, with the slope (alpha) serving as a proxy for the efficiency of *U. pinnatifida*'s photosystem II (PSII). Inspection of the multi-day time series of alpha revealed a significant decline in PSII efficiency under constant temperature, suggesting that the experimental setup was unable to maintain stable PSII performance. Therefore, the second hypothesis remains inconclusive regarding the response of *U. pinnatifida*'s PSII efficiency to warming. Nevertheless, Experiment 1 indicated the possibility of a positive response to moderate warming from 14 to 19 °C, and a negative response to further warming to 23 °C. This was also evident in Experiments 2 and 3, despite an overall decline in PSII performance including blade discoloration.

Our experiments highlight a critical measurement artefact that must be addressed before attempting to monitor PSII performance in the field. Seaweed blades should not remain fixed in position during unattended automated fluorometry. Instead, they should be mounted on the fluorometer only for the duration of an SP analysis. Although more labour-intensive, this approach enables adequate replication when the number of available PAM fluorometers is limited, and reduces confounding effects associated with prolonged blade immobilisation.

List of tables

List of figures

Introduction

Global climate change is driving unprecedented shifts in marine environments, notably in the seawater carbonate system (Zeebe 2012, Bushinsky et al. 2019), temperatures (Wernberg et al. 2011c), and oxygenation (Breitburg et al. 2018, Deutsch et al. 2024). Rising ocean temperatures can affect primary producers such as seaweed (Hoegh-Guldberg & Bruno 2010, Wernberg et al. 2011a, Smale et al. 2019). Among the most alarming developments is the increasing frequency and intensity of ocean heatwaves, which disrupt key physiological processes of marine organisms, including photosynthesis (Oliver et al. 2018). To classify these warming events, Hobday et al. (2016) defined ocean heatwaves as periods when sea surface temperatures (SSTs) exceed the 90th percentile of the climatological mean for at least five consecutive days. Using this definition, Oliver et al. (2018) demonstrated that ocean heatwaves have increased in both frequency (by 34%) and duration (by 17%) since the early 20th century. The primary factor driving this trend has been rising mean ocean temperatures (Frölicher et al. 2018, Oliver et al. 2018), with projections indicating that ocean heatwaves will likely intensify, become more frequent, and last longer as climate change continues (Frölicher et al. 2018).

Over the past four decades, more than 70% of the world's coastlines have experienced substantial warming (Lima & Wethey 2012), and projections indicate near-surface temperature increases of 2–7 °C by the end of the century (Christensen et al. 2007; Lima & Wethey 2012). Between 2011 and 2020, the average global ocean surface temperature rose by 0.88 °C (range: 0.68–1.01 °C) compared to the 1850–1900 baseline, with 0.60 °C (range: 0.44–0.74 °C) of this warming occurring since 1980. Future projections suggest additional increases of 0.86, 1.51, 2.19, and 2.89 °C under the Shared socio-economic pathways (SSPs): (SSP1-2.6, SSP2-4.5, SSP3-7.0, and SSP5-8.5 scenarios, respectively, relative to the 20-year period ending in 2014 (IPCC 2021). Since 1982, the occurrence of marine heatwaves has doubled, accompanied by notable increases in both their intensity and duration (Schoeman et al. 2021). Consequently, 46% of coastlines have experienced a significant decline in the frequency of cold days, while 38% have seen a rise in extreme hot days, defined as the surface seawater temperature (SSTs) exceeding the 95th percentile of standardised anomalies from 1982 to 2010 (Lima & Wethey 2012). Looking ahead, projections suggest that ocean heatwaves will become even more frequent over the next two decades, with a four-fold increase under the SSP1-2.6 scenario and an eight-fold increase under SSP5-8.5 (Schoeman et al. 2021).

These SSPs events are influenced by both local-scale processes, such as ocean heat advection and vertical mixing, and broader climate patterns like El – Nino (Holbrook et

al. 2019). Johnson et al. (2019) highlight the role of atmospheric circulation patterns, such as atmospheric blocking and El Niño events, in driving the formation of ocean heatwaves. For example, the global blocking patterns during summer can cause stagnant high-pressure systems, preventing cooler air masses from moving in, thereby prolonging intense ocean warming. Additionally, the accumulation of greenhouse gases traps heat, causing a long-term rise in SSTs and amplifying the frequency and severity of heatwave events (IPCC 2021).

Ocean heatwaves have profound ecological and socio-economic consequences (Madin et al. 2012, Pecl et al. 2017, Frölicher & Laufkötter 2018, Smale et al. 2019). They have triggered widespread coral bleaching (Couch et al. 2017, Hoegh-Guldberg & Poloczanska 2017, Le Nohaïc et al. 2017), the loss of kelp (a large brown cold-water seaweed) forests (Wernberg et al. 2016, Thomsen & South 2019, Thomsen et al. 2019), and increased stratification of ocean surface layers (Bond et al. 2015, Schaeffer & Roughan 2017). They have also caused mass mortality in marine invertebrates (Oliver et al. 2017), rapid range shifts in species with narrow tolerance such as kelps and cold-water fishes (Smale & Wernberg 2013), benthic community restructuring (Wernberg et al. 2013, Bennett et al. 2015), and fisheries closures (Caputi et al. 2016, 2019, Oliver et al. 2017).

Unlike gradual warming trends, marine heatwaves can exceed species' adaptive capacities, triggering sudden ecosystem shifts that are difficult to predict and manage (Scheffer & Carpenter 2003, Andersen et al. 2009, Wernberg et al. 2016). Such disruptions can result in severe economic losses, particularly for fisheries that depend on stable ecosystem functioning (Mills et al. 2013, Bennett et al. 2016, Caputi et al. 2016, Wernberg et al. 2019).

Seaweeds, or marine macroalgae, play a fundamental role in shallow-water rocky ecosystems, where they form extensive marine forests (Wernberg & Filbee-Dexter 2019). As primary producers and habitat-forming organisms, they support diverse communities and influence ecosystem structure worldwide (Dayton 1985, Tegner et al. 1997, Bertness et al. 1999, Wernberg et al. 2003, Buschbaum et al. 2006, Egan et al. 2014). Kelp forests, dominated by laminarian and fucalean seaweeds, are particularly important as they modify local environments and interact with adjacent habitats (Gaylord et al. 2007, Wernberg et al. 2018).

Most canopy-forming seaweed species such as kelp thrive in cool, nutrient-rich waters, making them vulnerable to warming and reduced water clarity (Fernandez 2011). Climate change over the past five decades has already shifted seaweed distribution and abundance (Lima et al. 2007, Wernberg et al. 2011b, Krumhansl et al. 2016, Filbee-Dexter & Wernberg 2018, Casado-Amezúa et al. 2019), with additional changes linked

to ocean heatwaves (Carballo et al. 2002, Vásquez et al. 2014, Reed et al. 2016, Wernberg et al. 2016, Thomsen et al. 2019).

Rising ocean temperatures affect seaweed populations both directly and indirectly. Physiologically, warming can induce sublethal stress, reduce growth, and increase susceptibility to other environmental pressures (Van den Hoek 1982, Kordas et al. 2011, Tuya et al. 2012, Wernberg et al. 2013). Indirect impacts include altered competition and increased grazing by range-expanding herbivores (Haraguchi et al. 2009, Ling et al. 2009, Vásquez et al. 2014, Bennett et al. 2015, Franco et al. 2017). Prolonged heat events, often combined with solar radiation, desiccation, and eutrophication, can push seaweeds beyond thermal tolerance limits, causing reproductive failure and local extinctions (O'Brien & Scheibling 2016, Straub et al. 2019, Wernberg et al. 2016, Smale et al. 2019).

The invasive kelp *Undaria pinnatifida* (Harvey) Suringar, 1873, is native to Asia but now colonises temperate coasts globally, often displacing native macroalgae (South et al. 2017). Its environmental tolerance and rapid growth make it a strong candidate for studying temperature effects on photosynthesis—a process essential for growth and reproduction. A key measure of photosynthetic performance is Photosystem II (PSII – is the first protein pigment complex of the photosynthetic electron transport chain responsible for capturing light energy to drive water photolysis and supply electrons for downstream photochemical processes) efficiency, which is sensitive to temperature change. While prolonged marine heatwaves have been shown to impair seaweed physiology and even cause local extinctions (Harley et al. 2012, Wernberg & Straub 2016, Smale et al. 2019), the species-specific PSII response of *U. pinnatifida* to acute and sustained warming remains poorly understood (Hurd et al. 2014, Thomsen et al. 2019).

Although there are numerous studies on seaweed responses to climate change (Krumhansl et al. 2016, Smale et al. 2019), relatively few examine how warming directly affects PSII photochemical efficiency in seaweed. Some have explored thermal tolerance and growth responses, but fewer have addressed PSII function—a central determinant of photosynthetic capacity (Hanelt et al. 1997, Takahashi & Murata 2008).

Photosynthetic response of seaweed species to warming

Seaweeds rely on photosynthesis to support growth and metabolic functions. Similar to terrestrial plants, their photosynthetic performance is influenced by environmental factors such as temperature. In many macroalgal species, moderate temperature increases within their thermal tolerance can enhance photosynthetic activity by accelerating enzymatic reactions (Davidson & Pearson 1996, Gao et al.2012, Terada et

al. 2020). However, temperatures exceeding the optimal threshold often led to photoinhibition or irreversible photodamage to PSII, resulting in reduced photosynthetic efficiency (Hanelt et al. 1997, Davison & Pearson 1996, Kumar et al. 2020, Roleda 2009).

Thermal tolerance varies not only among macroalgal species and among populations of the same species, often reflecting differences in local acclimation history and environmental conditions (Mccoy & Widdicombe 2019). While some seaweeds exhibit short-term protective responses to heat stress—such as enhanced non-photochemical quenching (NPQ)—these mechanisms are often insufficient to prevent chronic damage to PSII function (Koch et al. 2013). The species *U. pinnatifida* has shown sensitivity to thermal stress, particularly under prolonged or repeated exposure to elevated temperatures (Barrento et al. 2016). As marine heatwaves become more frequent under climate change, understanding species-specific photosynthetic responses is essential for predicting shifts in macroalgal distribution and community structure.

Experimental approaches and methodological context

Controlled laboratory experiments are widely employed to investigate the photosynthetic responses of seaweeds to temperature fluctuations (Wernberg et al 2016). These studies typically involve collecting live specimens, acclimating them to laboratory conditions, and then subjecting them to various temperature treatments over a defined period. To accurately isolate the effects of temperature, other environmental variables such as light intensity, photoperiod, salinity, and nutrient availability are either maintained at constant levels or deliberately manipulated to assess potential interactions (Eggert 2012).

A critical component of such experimental setups is the acclimation period, during which specimens are maintained at baseline temperatures to ensure physiological stability prior to thermal treatments. During this phase, a stable value of the initial slope (α) of the relationship between photosynthetically active radiation and the photosynthetic electron transport rate (hereafter, PAR–ETR curve) should be established, indicating successful acclimation. A continued decline in α values may signal physiological stress, potentially caused by suboptimal tank conditions, nutrient limitation, inadequate water circulation (Franklin & Forster 1997), or even issues with the fluorometric measurement itself. These methodological limitations must be acknowledged, as they can confound interpretation of results.

Temperature effects on seaweed photosynthesis are often studied under controlled laboratory conditions using Rapid Light Curves (RLCs). This method involves exposing the organism to a rapid stepwise sequence of increasing ambient PAR, with a saturation pulse (SP) applied at each step to assess PSII performance (Schreiber 2004). While

RLCs enable quick assessment of photosynthetic parameters, they represent an artificial and non-natural mode of light exposure.

As an alternative, a time series of SP analyses could be conducted—e.g., at 30-minute intervals—over the course of one or several days, allowing ETR to be assessed in relation to the natural diel cycle of PAR. If automated and performed *in situ*, this approach could capture PSII responses to real-time environmental fluctuations, such as those occurring during a natural heatwave (Beer et al. 2000). Automation of such time-series measurements requires that the seaweed—naturally exposed to turbulent flow—remains attached to the fluorometer throughout the monitoring period.

The use of automated PAM fluorometry

Pulse-Amplitude Modulation (PAM) fluorometry is a widely adopted method for assessing *in vivo* PSII photochemical efficiency in photosynthetic organisms, including macroalgae (Beer and Axelsson 2004). The technique provides non-invasive and real-time measurements of chlorophyll fluorescence, enabling continuous monitoring of photosynthetic performance under various environmental conditions (Schreiber 2004). Automated PAM systems are particularly useful in long-term monitoring, allowing unattended measurements.

This automation for unattended measurements requires the organism of interest to remain at a fixed distance in front of the fluorometer, making the setup generally suitable for sessile organisms such as corals and coralline algae (e.g. Li et al. 2024, McNie et al. 2025). However, for organisms like seaweeds that exhibit continues movement, such positioning may be detrimental, potentially altering their physiological state. Whether seaweeds can be held stationary in front of a PAM fluorometer without inducing negative physiological effects remains uncertain.

Here, we evaluated the feasibility of such approach under controlled laboratory conditions. We trialled unattended, automated PAM fluorometry to determine whether such measurements could be applied in the field to monitor seaweed PSII performance during natural heatwaves.

This study addresses two main questions:

1. Can *U. pinnatifida* remain attached to the PAM fluorometer for extended periods without compromising its photosynthetic performance, thereby enabling automated in situ measurements?

2. How does PSII photochemical efficiency in *U. pinnatifida* respond to experimental warming designed to simulate marine heatwave conditions?

Material and methods

Experimental design

We conducted three laboratory experiments with the invasive seaweed *Undaria pinnatifida* and a controlled diel light cycle to investigate whether an experimental setup for unattended automated PAM fluorometry can (1) ensure stable performance of the seaweed's PSII, and (2) reveal how seawater warming effects this performance. In each experiment, seawater temperatures were increased following an initial acclimation period at 14–15 °C, reaching 19 and 23 °C in Experiment 1, 18 °C in Experiment 2, and 22 °C in Experiment 3.

To measure the efficiency of the seaweed's PSII, we used a Monitoring PAM (Walz GmbH, Germany) with three (Experiment 1) or six (Experiments 2 and 3) fluorometer heads. The PAM fluorometers generated a continues time series of saturation pulse analyses at 30-minute intervals, revealing the relative ETR (rETR) as a function of PAR.

To evaluate changes in the PSII efficiency, we plotted rETR against PAR for each five-hour period following the daily onset of light, and then assessed the evolution of the slope of the resulting curve, α, during the acclimation period and the subsequent warming phase.

Experiment 1

Experiment 1 ran for 26 days, from 23 September to 18 October 2023. One specimen of *U. pinnatifida* was placed in each of three seawater recirculation units (hereafter, tanks) as shown in Figure 1A. Unlike in Experiments 2 and 3 (see below), only three PAM measuring heads were available, preventing replication of measurements within each tank.

The seawater in all tanks was maintained at 15 °C for an initial 14-day acclimation period. Following this, the temperature was increased to 19 °C in one tank and to 23 °C in another, while the third tank remained at 15 °C and served as the control.

For fluorometric time-series measurements, a single seaweed blade was held at a fixed distance from the fluorometer by a sample clip (Fig. 1B). This blade was replaced six times during the experiment with a neighbouring blade of the same individual.

Experiments 2 and 3

Experiments 2 and 3 ran 13 and 9 days, respectively, during September and October 2024. Here, we used two tanks, each containing three *U. pinnatifida* specimens as

shown in Figure 2. The specimens were acclimated at 14 °C, although for different durations: 10 days in Experiment 2 and two days in Experiment 3. Following acclimation, the temperature in one of the two tanks was gradually increased—to 18 °C over three days in Experiment 2, and to 22 °C over six days in Experiment 3.

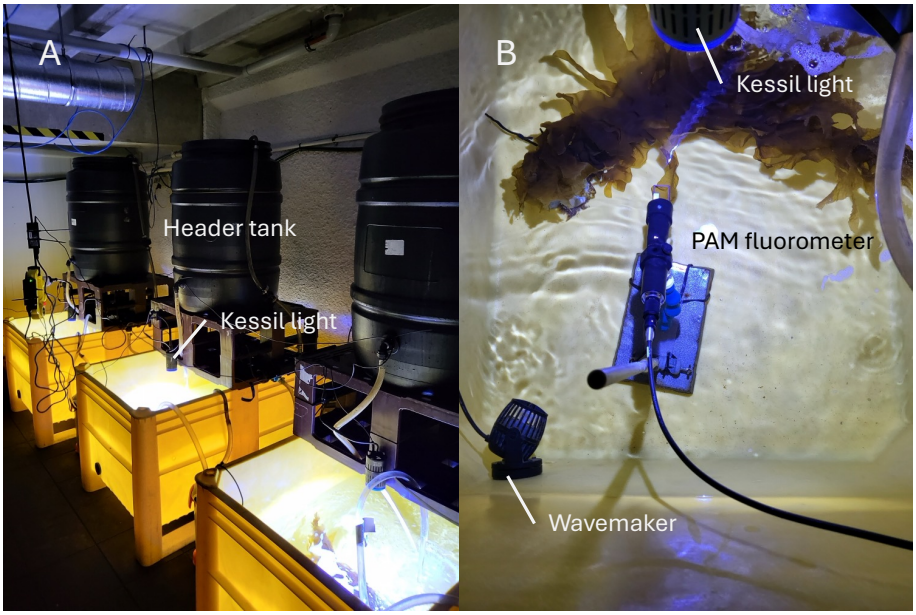

Figure 1. Laboratory setup for Experiment 1. (A) Photograph showing three seawater recirculation units each consisting of a yellow 600 L tank and a black header tank. One A160WE Tuna Blue Kessil light provided photosynthetically active radiation as specified in Figure 4. (B) One PAM fluorometer measuring head attached to an *Undaria pinnatifida* blade. Shown is also a wavemaker agitating the seawater in the tank.

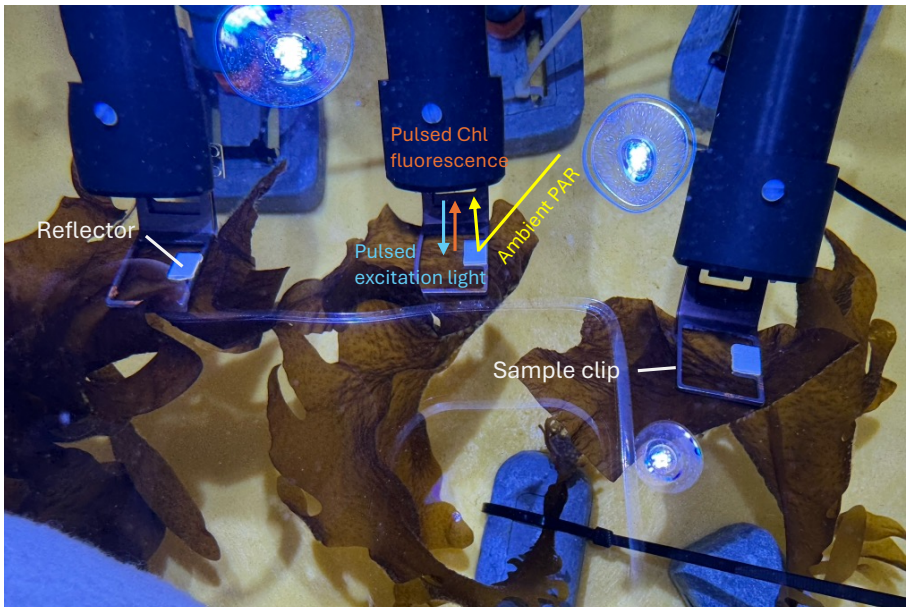

Figure 2. Measurement setup for Experiments 2 and 3. Photograph showing three submerged PAM fluorometer heads each attached to a blade of an *Undaria pinnatifida* specimen. The sample clip keeps the blade at a fixed distance for 30-minute interval saturation pulse analyses. The reflector enables the measurement of the intensity of the ambient light by an internal light sensor. The fluorometers emit pulsed excitation light to measure the resulting pulsed chlorophyll fluorescence.

Specimen collection

Individuals of *U. pinnatifida* were collected from floating docks of the Orakei Marina, near Okahu Bay (36° 50'58.8''S, 174° 48'35.6''E), located in the suburb of Orākei on the eastern coastline of Auckland, New Zealand (Fig. 3).

Okahu Bay, situated at the mouth of the Waitematā Harbour, is a sheltered embayment influenced by both tidal marine waters and freshwater runoff from nearby urban catchments. The bay features sandy and muddy substrates, with patches of rocky intertidal areas. Salinity levels in Okahu Bay range from 28 to 34, depending on rainfall and tidal cycles. Surface water temperatures fluctuate between 14 °C in winter and up to 22 °C in summer.

Individual specimens of *U. pinnatifida* were cut off the sides of the docks and stored in a refrigerated container for transport to the marine laboratory of Auckland University of Technology. In the laboratory, individuals were cable tied to a 1 kg lead weight at the stipe and placed at the bottom of their respective seawater tanks as shown in Figure 2.

Figure 3. Map showing the location of the seaweed collection site at the mouth of the Waitemata Harbour, Auckland, New Zealand (yellow star). © OpenStreetMap and other data providers, Apple Inc. The blue circle indicates the location of the AUT Marine Laboratory.

Laboratory setup

Each experimental unit circulated ~500 litres of seawater, supplied by the NIWA Northland Marine Research Centre in Ruakākā, New Zealand. There, the seawater was pumped from Bream Bay, sand-filtered, sterilised by exposure to UV light, and then filled into a seawater trailer for transport to the laboratory in Auckland (a process employed by NIWA)

The seawater circulation units consisted of a 112 × 72 × 60 cm main tank and an elevated 210 L header tank (Fig. 1A). A pump (Eheim 1260 Universal Pump) submerged in the main tank moved seawater at a rate of ~9 litres min^{-1} through an external chiller (Hailea HC-300A) and a UV sterilizer (Pond One UV-C 9W, Clear Tec) into the header tank, from which the seawater returned to the main tank by gravity. A heater (500 W GH Quartz Glass heater, Aqua One) was placed on the floor of the main tank to aid temperature control. Furthermore, an external particle filter (Professional 4+ 350 Cannister filter, Eheim) circulated the seawater in the main tank to remove suspended particles. A wavemaker attached to the side wall of the main tank in all experiments(Fig. 1B) generated pulsed jets to keep the seaweed in motion, and one (Experiment 1), three (Experiments 2), or four (Experiment 3) Kessil Tuna Blue LED lights linked to a Spectral Controller provided daily cycles of PAR.

Data acquisition

The seawater salinity was manually measured daily using a conductivity meter (Knick GmbH) and maintained at 34.5 by addition of reverse osmosis water.

To assess the photosynthetic performance of *U. pinnatifida*, a PAM fluorometry system was used, comprising of three (Experiment 1, one in each tank) or six (Experiments 2, 3; three in each tank) MONI-HEAD/485 measuring heads. In Experiment 1, these measuring heads were connected to a MONI-IB4/USB PC interface box (Heinz Walz GmbH, Germany) as shown in Figure 4A. The interface was connected to a laptop PC running WinControl-3 software, which executed a measurement routine (see below in figure 4) and recorded the data.

In Experiments 2 and 3, on the other hand, the measuring heads were connected to a MONI-DAS/S Data Acquisition System, which executed the measurement routine, recorded the resulting data, and transmitted data in real time to a cloud server via a Wi-Fi modem (Fig. 4B). In these experiments, a laptop PC running WinControl-3 software was connected only at the start of the time series measurements to test the correct functioning of the measuring heads and upload the measurement routine in form of a batch file.

MONI-HEAD/485 Measuring Head

The MONI-HEAD/485 is a water-tight plastic cylinder (30 mm diameter, 280 mm length) designed for submerged operation in aquatic environments (Figs. 1B, 2). It detects fluorescence with a PIN-photodiode featuring a long-pass filter (50% transmittance at 645 nm) and a selective window amplifier. The measuring head used a blue power LED (peak wavelength 470 nm) to emit measuring light pulses and actinic light. An internal

photodiode, protected by near-infrared filter, measured the PAR reflected by a white 13 × 7 mm optically diffuse Teflon sheet. Furthermore, the circuit board of the measuring head included a temperature sensor to monitor the temperature of the ambient seawater in real-time.

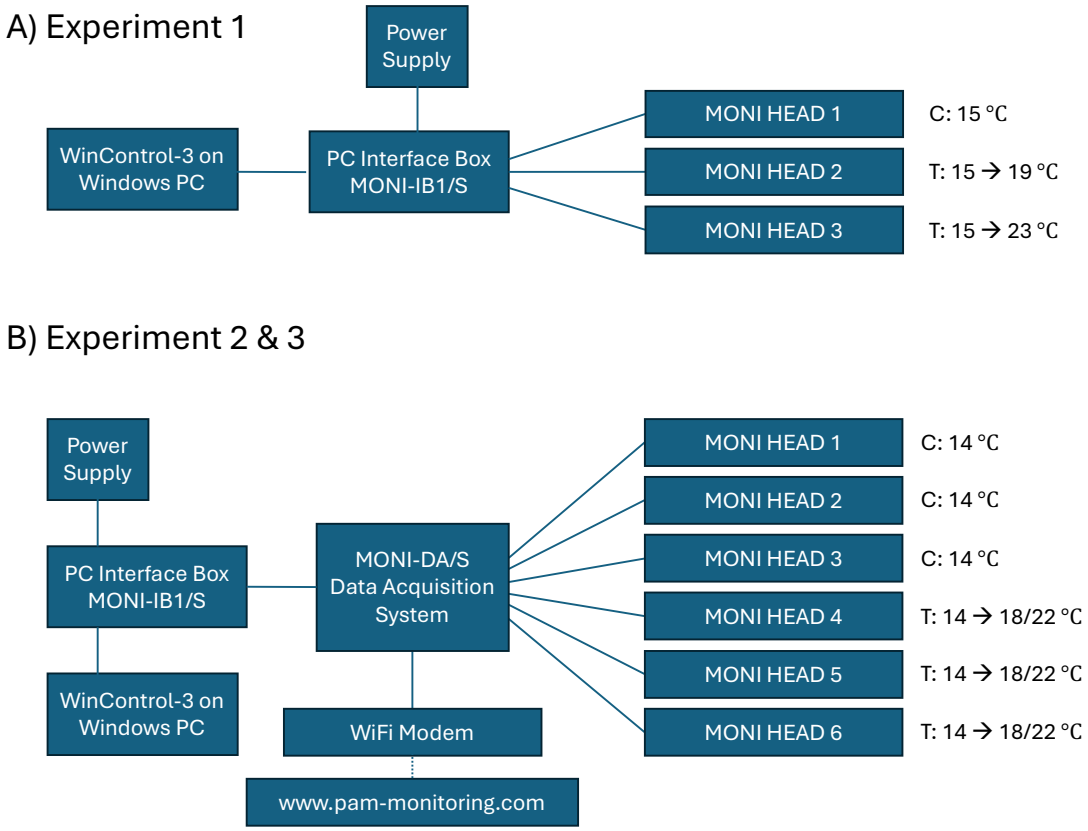

Figure 4. PAM fluorometer setup for Experiments 1–3. (A) In Experiment 1, three PAM measuring heads were connected to a PC interface box and a laptop computer. (B) In Experiments 2 and 3, six PAM measuring heads were connected to a MONI-DAS/S underwater data acquisition system. The MONI-DA/S recorded all data and transferred data via WiFi modem to a server in real time. At the start of the experiment, the MONI-DA/S was connected to a laptop running Win-Control-3 software to configure the measuring heads and to upload a batch file for automated time-series saturation pulse analyses.

To correctly position the seaweed blade for fluorescence measurements, each measuring head was equipped with a sample clip made of two aluminium frames (35 × 25 mm), pressed together by an O-ring and positioned 25 mm from the optical window of the PAM measuring head (Fig. 2). The clip was mounted at a 120° angle relative to the measuring head's optical axis.

Fluorescence measurement

Fluorescence measurements were automated using a custom batch script designed to control the timing of PAM fluorometer's SP analyses. The script utilised a looping structure to continuously execute programmed measurement steps as follows:

Each day, the script initiated an F_0/F_m (the baseline fluorescence ratio) determination at 19:00 (7:00 PM), to derive the maximum quantum yield of PSII photochemistry in darkness (Table 1). Subsequently, from 19:30 (7:30 PM) through to 18:30 (6:30 PM) the following day, saturation pulse analyses were conducted at 30-minute intervals. At each time point, the measuring light was activated 20 seconds before the saturation pulse, which reached an intensity of 1500 µmol photon m^{-2} s^{-1}. Once the saturation pulse analyses was completed, the measuring light was switched off until the next interval.

Table 1: Measured and derived fluorescence parameters.

Fluorescence parameter	Symbol	Equation/comments	Reference
Minimum fluorescence in dark-adapted state	F_0	Measured in darkness	
Maximum fluorescence in dark-adapted state	F_m	Saturation pulse	
Variable fluorescence	F_v	$F_m - F_0$	
Fluorescence in the presence of actinic light	F		
Maximum fluorescence in the presence of actinic light	F_m'	Saturation pulse	
Maximum photochemical quantum yield of PSII	F_v/F_m	$(F_m - F_0) / F_m$	Kitajma & Butler 1975
Effective photochemical quantum yield of PSII	Y(II)	$(F_m' - F) / F_m'$	Genty et al. 1989
Relative electron transport rate	rETR	$Y(II) \times PAR \times 0.85 \times 0.5$	Klughammer & Schreiber 2008

Data analysis

PSII performance

The fluorescence returned from the emitted pulses of measuring light was used to measure and derive the following parameter (Table 1):

In darkness (dark-adapted state)

1) Measured: PSII steady–state fluorescence of a dark-adapted seaweed blade, measured in darkness (F_0),
2) Measured: PSII maximum fluorescence (F_m) of a dark-adapted seaweed blade during a saturation pulse of actinic light,
3) Derived: PSII variable fluorescence of a dark-adapted seaweed blade ($F_v = F_m - F_0$),
4) Derived: PSII maximum quantum yield of a dark-adapted seaweed blade (F_v/F_m),

Under conditions of actinic light

5) Measured: PSII steady-state fluorescence under conditions of actinic light (F),

6) Measured: PSII maximum fluorescence of a seaweed blade adapted to actinic light, during application of saturating pulse (F_m'),

7) Derived: PSII effective quantum yield under conditions of actinic light (Y(II) = (F_m' – F) / F_m'),

8) Derived: Relative electron transport rate (rETR = Y(II) × $E_{(PAR)}$ × 0.85 × 0.5): Yield (with or without actinic light) multiplied by PAR, absorption factor, and factor 0.5 to account for the assumption that absorbed photons are equally distributed between PSII and PSI.

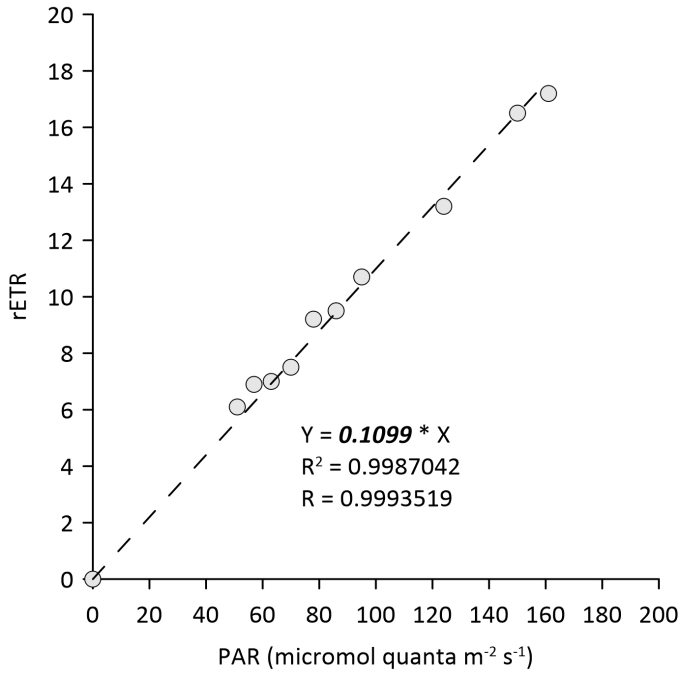

Figure 5. Example analyses of the PSII photosynthetic efficiency of an *Undaria pinnatifida* blade. The diel series of 30-minute interval saturation pulse analyses were used to calculate and plot rETR as a function of PAR. Note that only measurements conducted during increasing PAR were considered. The slope of the linear fit is used as a measure of PSII efficiency.

The performance of PSII was assessed by examining the relationship between rETR and incident PAR. Specifically, we calculated alpha (α), the slope of the linear regression of the rETR versus PAR curve, using only the saturation pulse analyses conducted during the first five hours after the onset of light each day as shown in Figure 5. All other analyses were excluded to avoid the confounding effects of hysteresis. The daily α values were then plotted as a time series to visualise trends in PSII efficiency over the course of each experiment.

Statistical data analysis

To assess temporal changes and differences between the seaweed specimens submerged in the two Tanks during Experiment 2 (acclimation period only) and

Experiment 3 (treatment period only), we employed linear mixed-effects modeling using the *lme4* package in R (version 4.5.1). This approach accounts for repeated measures within individuals and allows for flexible modeling of fixed and random effects.

Separate models were fitted for Experiment 2 and Experiment 3 datasets. In each model, the response variable was modeled as a function of Time, Tank, and their interaction, with individual ID included as a random effect to account for within-subject variability.

Models were fitted using restricted maximum likelihood (REML). Fixed effects were evaluated using *t*-values, with approximate *p*-values derived from the normal distribution. Model assumptions (normality, homoscedasticity) were checked via residual diagnostics.

A significant Time effect indicates a consistent change in alpha over time. A significant Tank effect reflects baseline differences between experimental groups. A significant Time × Tank interaction suggests that the rate of change in alpha differs between groups.

Results

Experiment 1

Acclimation period

In Experiment 1, the three specimens of *Undaria pinnatifida* were acclimated under conditions of a stable ambient temperature ranging from 14.5–15.5 °C for the first 14 days (Table 2).

Throughout the experiment, these specimen received 13.5 hours (05:00–18:30 h) of photosynthetically active radiation (PAR) each day, with a mid-day peak of ~44 μmol quanta m^{-2} s^{-1} as shown in Figure 6.

The fluorometric measurements, which started on day 10, 23 September 2023 (Table 2), revealed that the daily α values, derived from the analyses of ten saturation pulses delivered during the first five hours after the onset of light each day, gradually declined over the following four days by 0.063 units in Tanks 1 and 2, and 0.077 units in Tank 3 (Fig. 8, Table 2). Tank 1 is the control tank across all experiments.

Following these initial measurements, we replaced the blades in the sample clip of the PAM fluorometers in each of three tanks and raised the temperature in Tanks 2 and 3 to 19 and 23 °C, respectively (Fig. 7).

Table 2: *Undaria pinnatifida*. Summary of Experiment 1 data including α, the initial slope of the rETR versus PAR curve, and T, the seawater temperature (°C).

	Tank 1		Tank 2		Tank 3	
Date	α	T	α	T	α	T
Blade 1						
23 Sep 23	0.233	14.8	0.228	15.3	0.226	15.4
24 Sep 23	0.213	14.8	0.206	15.2	0.214	15.1
25 Sep 23	0.197	14.7	0.190	15.2	0.196	15.5
26 Sep 23	0.176	14.9	0.177	15.3	0.165	15.1
27 Sep 23	0.170	14.5	0.165	15.5	0.149	15.1
Blade 2						
27 Sep 23	0.241	14.5	0.265	18.5	0.258	15.1
28 Sep 23	0.242	15.1	0.275	19.3	0.259	21.5
29 Sep 23	0.233	14.7	0.285	19.4	0.260	23.2
30 Sep 23	0.223	14.7	0.277	19.3	0.253	23.2
01 Oct 23	0.210	15.2	0.283	19.5	0.246	23.3
Blade 3						
01 Oct 23	0.270	15.2	0.271	19.6	0.257	23.3
02 Oct 23	0.237	14.7		19.5	0.226	23.2
03 Oct 23	0.232	14.9	0.263	19.4	0.209	23.2
04 Oct 23	0.218	15.0	0.265	19.4	0.203	23.4
05 Oct 23	0.210	15.0	0.256	19.3	0.218	23.4
06 Oct 23	0.187	14.6	0.243	19.3	0.233	22.9
Blade 4						
06 Oct 23	0.239	14.6	0.277	19.4	0.249	22.9
07 Oct 23	0.215	14.8	0.268	19.4	0.210	22.3
08 Oct 23	0.197	14.7	0.260	19.0	0.175	22.3
09 Oct 23	0.182	15.0	0.258	19.3	0.142	23.1
10 Oct 23	0.161	14.7	0.247	19.3	0.120	23.3
Blade 5						
10 Oct 23	0.280	14.7	0.266	19.4	0.265	23.3
11 Oct 23	0.232	14.9	0.265	19.4	0.254	23.3
12 Oct 23	0.215	14.8	0.260	19.4	0.239	23.1
13 Oct 23	0.231	14.7	0.266	19.4	0.254	23.1
14 Oct 23	0.195	14.8	0.236	19.4	0.234	23.2
15 Oct 23	0.183	14.8	0.216	19.4	0.221	23.1
Blade 6						
15 Oct 23	0.231	14.8	0.264	19.4	0.264	23.1
16 Oct 23	0.230	14.7	0.245	19.4	0.240	23.1
17 Oct 23	0.218	14.8	0.239	19.5	0.224	23.3
18 Oct 23	0.211	14.7	0.222	19.5	0.202	23.2

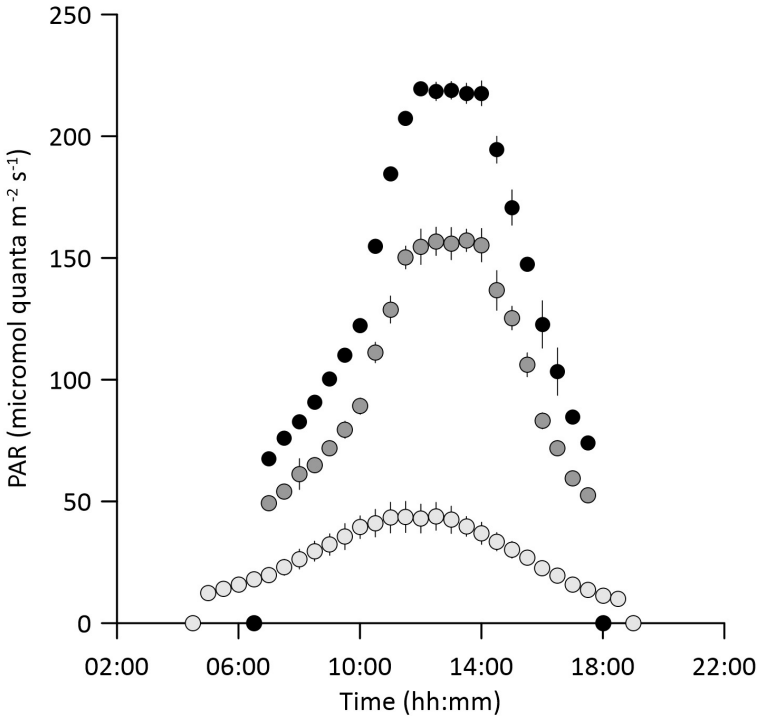

Figure 6. Diel variations in the intensity of the photosynthetically active radiation (PAR, Mean +/– SD) incident at the surface of *Undaria pinnatifida* blades during Experiment 1 (light grey, n = 27), Experiment 2 (grey, n = 13), and Experiment 3 (black, n = 8).

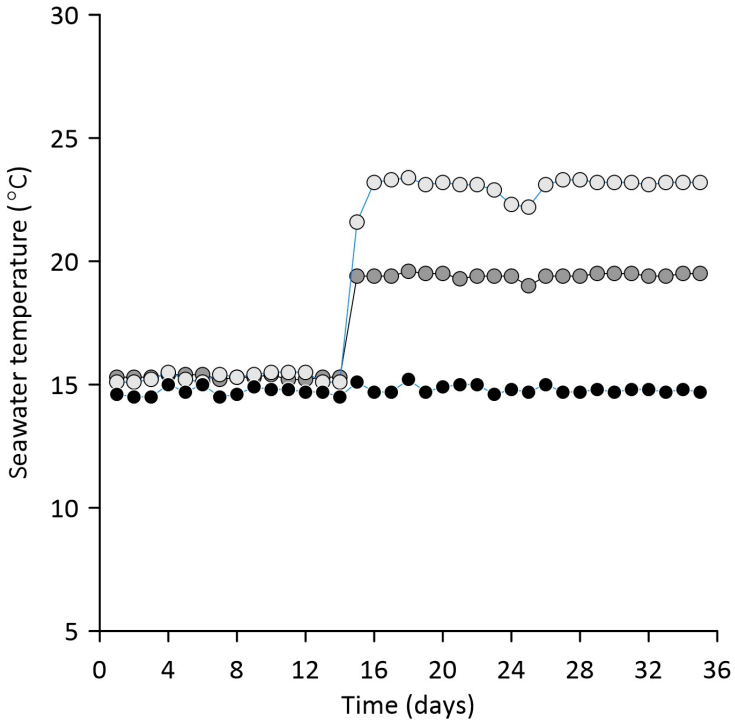

Figure 7. Experiment 1. Time series of seawater temperatures measured in each of three tanks. Black, Control; Grey shades, Treatments.

Initial response to warming

The new blade of the specimen that remained at ~15 °C in Tank 1 exhibited an α value of 0.24 for the first two days, which was 3.4% higher than that of the blade measured during the initial acclimation period. Thereafter, the α value decreased to 0.21 over three days confirming the trend of decreasing α observed during the initial acclimation period.

In contrast, the α values of the specimen in Tank 2 increased to ~114% of that in Tank 1(control tank) (15 °C) as the temperature reached 19.3 °C on the second day of this measurement period (Table 2). Thereafter, α remained at ~0.28 over the following three days.

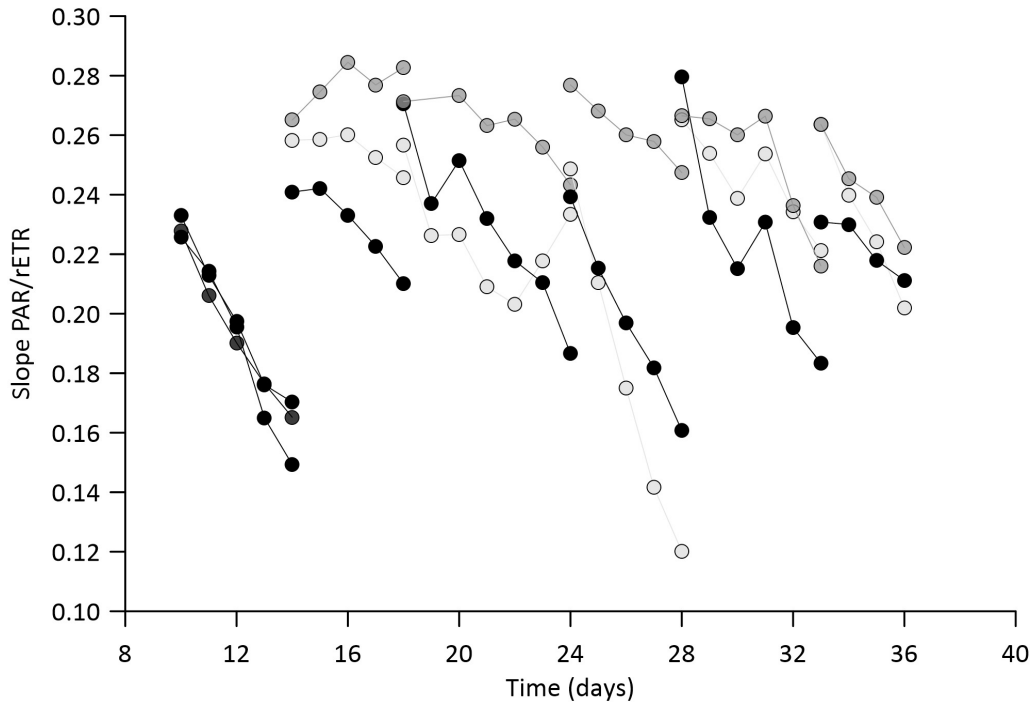

Figure 8. Experiment 1. Time series of alpha, the slope of the initial rETR–PAR curve, derived from daily 30-minute interval saturation pulse analyses at ambient seawater temperatures of 15 (black), 19 (grey), and 23 °C (light grey). Six blades were measured consecutively, in each of three tanks.

The α value of the blade measured in Tank 3, on the other hand, increased from 0.258 to 0.260 as the temperature increased from 15 to 23 °C, and then, as observed in 15 °C seawater, decreased over the remaining two days.

Overall, the data of the second measurement period (Fig. 8) indicate that the gradual increase in seawater temperature in Tanks 2 and 3, from 15 °C to 19 and 23 °C, respectively, had increased the initial differences in the α values between the Control (15 °C) and the Treatment (19 and 23 °C). At the end of the five day measurement

period, the α value of the blade in 23 °C was 17% higher, and that in 19 °C was 35% higher than that measured in 15 °C.

Trends over 21 days

The subsequent four consecutive measurement periods, each starting with a new blade of the respective *U. pinnatifida* specimen, revealed that (1) the α values of newly attached blades gradually decreased over the following 3–5 days in all temperature treatments, and (2) the α values of blades in 19 °C seawater was generally higher than those measured in 15 and 23 °C.

By the end of the experiment, after 36 days, the differences in the observed α values between 19 and 23 °C temperature treatments had decreased and the α values of blades in 15 °C seawater remained below those observed in warmer seawater.

Experiment 2

The six *U. pinnatifida* specimen tested in Experiment 2 received 10.5 h of PAR each day (07:00–17:30 h) with a mid-maximum of 157 µmol quanta m^{-2} s^{-1} as shown in Figure 6. The temperature of the seawater in the two tanks, Control and Treatment, was maintained at ~14 °C for 10 days (Table 3, Fig. 9).

Overall, the α values derived from the time-series saturation pulse analyses gradually declined in both tanks for all six specimens, by up to >50% as illustrated in Figure 9. This decline was accompanied by a gradual blade discoloration.

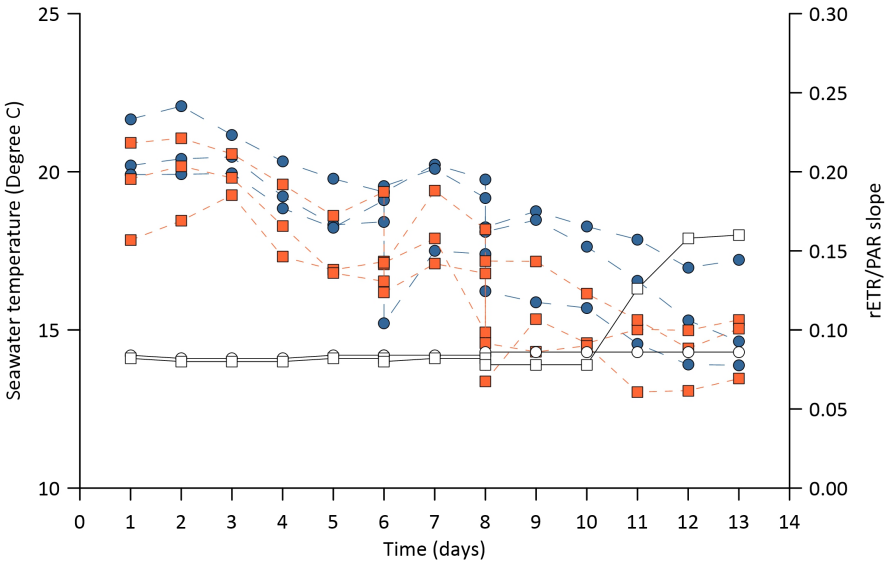

Figure 9. Experiment 2. Time series of alpha, the slope of the initial rETR–PAR curve, derived from daily 30-minute interval saturation pulse analyses at 14 °C (Control, blue symbols, 13 days), and initially 14 (10 days) and then 18 °C (3 days, orange symbols). Open symbols, ambient seawater temperature in the Control and Treatment tank.

Acclimation period

Linear mixed-effects modeling of the data collected during the 10-day acclimation period revealed a significant main effect of Time (β = –0.046, t = –4.19), confirming that alpha declined over time (Table 3). The main effect of Tank was not statistically significant (β = –0.244, t = –1.03), but the interaction between Time and Tank was significant (β = –0.034, t = –2.26), suggesting that α values of specimens in Tank 2 experienced a steeper decline compared to α values of specimens in Tank 1. These results indicate that while specimens in both Tanks showed a downward trend, those in Tank 2 not only started with lower alpha but also deteriorated more rapidly over time.

Table 3: *Undaria pinnatifida*. Summary of Experiments 2 and 3 data including α, the initial slope of the rETR versus PAR curve, and T, the seawater temperature (°C).

	Control				Treatment			
		α		T		α		T
Date	Sp1	Sp2	Sp3	(ºC)	Sp4	Sp5	Sp6	(ºC)
Experiment 2: Warming to 18 °C								
11 Sep 24	0.204	0.198	0.233	14.2	0.157	0.196	0.218	14.1
12 Sep 24	0.208	0.198	0.242	14.1	0.169	0.204	0.221	14.0
13 Sep 24	0.209	0.199	0.223	14.1	0.185	0.196	0.211	14.0
14 Sep 24	0.185	0.177	0.207	14.1	0.146	0.166	0.192	14.0
15 Sep 24	0.166	0.165	0.196	14.2	0.138	0.136	0.172	14.1
16 Sep 24	0.168	0.182	0.187	14.2	0.143	0.131	0.187	14.1
17 Sep 24	0.205	0.150	0.202	14.2	0.188	0.158	0.142	14.1
18 Sep 24	0.195	0.148	0.183	14.2	0.164	-	0.136	14.1
19 Sep 24	0.175	0.170	0.118	14.3	0.107	0.143	0.086	13.9
20 Sep 24	0.165	0.153	0.114	14.3	0.092	0.123	0.090	13.9
21 Sep 24	0.157	0.131	0.091	14.3	0.100	0.106	0.061	16.3
22 Sep 24	0.139	0.106	0.078	14.3	0.100	0.088	0.062	17.9
23 Sep 24	0.144	0.093	0.078	14.3	0.106	0.101	0.069	18.0
Experiment 3: Warming to 22 °C								
19 Oct 24	0.203	0.227	0.208	14.3	0.206	0.195	0.180	13.9
20 Oct 24	0.195	0.228	0.201	14.3	0.202	0.188	0.170	13.9
21 Oct 24	0.204	0.228	0.207	14.3	0.212	0.198	0.172	15.5
22 Oct 24	0.181	0.219	0.194	14.3	0.204	0.183	0.160	18.1
23 Oct 24	0.157	0.202	0.174	14.3	0.196	0.154	0.125	19.1
24 Oct 24	0.140	0.186	0.166	14.3	0.182	0.153	0.110	20.2
25 Oct 24	0.113	0.159	0.140	14.3	0.174	0.128	0.088	21.1
26 Oct 24	0.094	0.132	0.115	14.2	0.145	0.116	0.051	22.5
27 Oct 24	0.075	0.110	0.095	14.2	0.126	0.093	0.050	22.3

Warming period

The increase in the temperature of the seawater in the Treatment tank from 14 to 18 °C appeared to halt this trend as the α values of the three specimens did not further decrease over the following three days, while those of the specimens in the Control tank continued to decline (Table 4, Fig. 9).

The experiment was stopped at this point as the discoloration of the blades indicated that the specimens were in poor health.

Table 4. Summary of statistical model results for Experiments 2 and 3. SE, standard error; ~*p*-value, approximate *p*-value derived from the normal distribution.

Effect	Estimate	SE	*t*-value	~ *p*-value
Experiment 2: 10 days acclimation				
Intercept	0.193	0.168	1.15	0.26
Time	-0.046	0.011	-4.19	<0.001
Tank	-0.244	0.237	-1.03	0.31
Interaction (Time × Tank)	-0.034	0.015	-2.26	0.03
Experiment 3: 9 days treatment				
Intercept	0.213	0.021	10.1	<0.001
Time	-0.020	0.002	-8.6	<0.001
Tank	-0.030	0.030	-1.0	0.32
Interaction (Tank × Day)	-0.010	0.003	-3.3	0.001

Experiment 3

Like in Experiment 2, the six *U. pinnatifida* specimen tested in Experiment 3 received 10.5 h of PAR each day (07:00–17:30 h). The mid-maximum of 219 µmol quanta m^{-2} s^{-1}, however, was 39% higher than that supplied in Experiment 2 (Fig. 6).

In Experiment 3, we shortened the initial acclimation period to two days and then gradually raised the temperature from 14 to 22 °C in one of the two tanks (Fig. 10). During the first three days (19–21 October), the α values derived for all six specimens tested remained stable, followed by a steep decrease over the following six days.

The graph in Figure 10 suggests that the gradual increase of the seawater temperature in the Treatment tank did not affect this trend. By Day 9 of the experiment, the α values for the three specimens in each of Control and Treatment were similar and had decreased to 37, 49, 46, and 61, 48, and 28% of their initial value (Table 3).

Statistical data analysis (excluding the acclimation period) revealed a significant main effect of Time (β = –0.020, t = –8.6), indicating a consistent decline in α values over time. The main effect of Tank was not statistically significant (β = –0.030, t = –1.0). However, the Time × Tank interaction was significant (β = –0.010, t = –3.3), suggesting that specimens in Tank 2 (Treatment) experienced a steeper decline in α values than those in Tank 1.

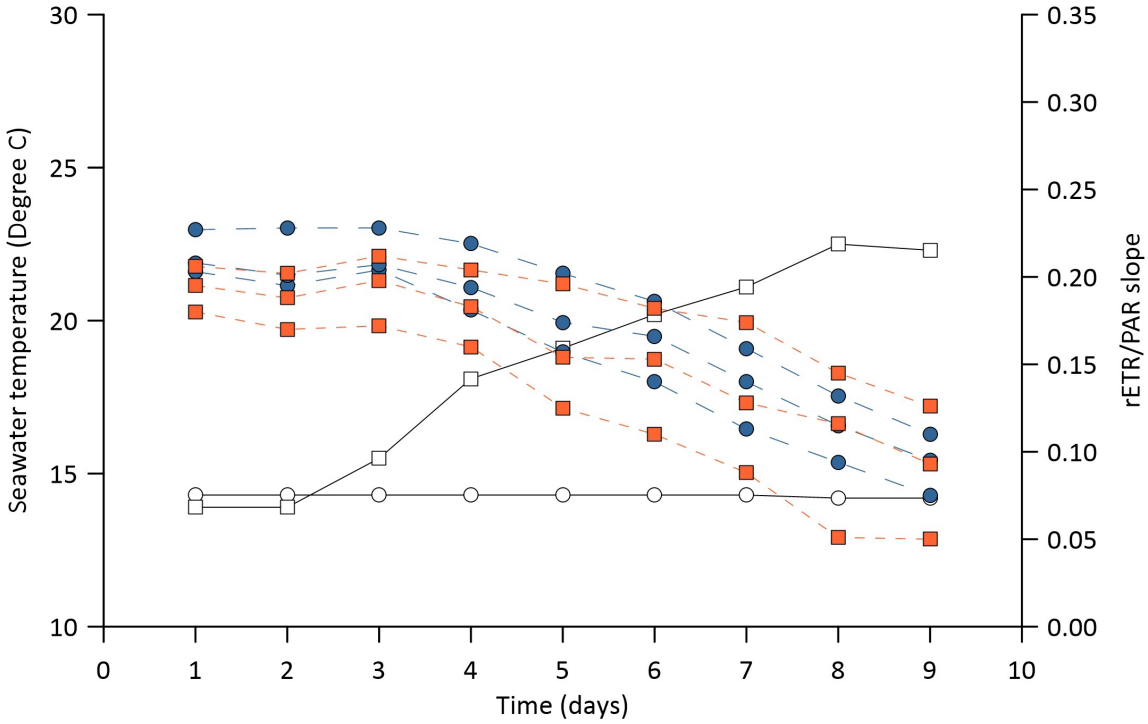

Figure 10. Experiment 3. Time series of alpha, the slope of the initial rETR–PAR curve, derived from daily 30-minute interval saturation pulse analyses at 14 °C (Control, blue symbols, 9 days), and initially 14 (2 days) and then gradually increasing up to 22 °C (orange symbols). Open symbols, ambient seawater temperature in the Control and Treatment tank.

Discussion

This study investigated the use of unattended automated PAM fluorometry to assess how the photochemical efficiency of *Undaria pinnatifida*'s PSII responds to experimental warming. The study had two objectives:

1. To evaluate whether the experimental setup could maintain stable PSII performance reflected by stable alpha (α) values under constant temperature conditions.

2. To examine whether gradual warming affects the efficiency of PSII in *U. pinnatifida*.

PSII performance under constant conditions

Unattended and automated *in situ* monitoring of PSII efficiency in seaweeds requires mounting a blade in front of the PAM fluorometer at a fixed position. To evaluate whether this setup can maintain stable PSII performance under constant conditions, three laboratory tests were conducted, each beginning with an acclimation period.

Throughout the initial acclimation phase, specimens in all three experiments were maintained under constant conditions: a temperature of 14–15 °C, moderate seawater

agitation, and a consistent diel light cycle. Under these conditions, we expected the photosynthetic performance quantified as the slope of the PAR/rETR curve to stabilise. However, this expectation was not met. Instead, α values consistently declined over time. This decline indicated that either (1) holding the blades in a fixed position negatively affected the blade's photosynthetic performance, and/or (2) inorganic nutrient concentrations in the seawater became limiting. Because replacement of blades in Experiments 1 reset the trend of decreasing PSII performance (Fig. 8), we can assume that the freely moving blades did not experience the decline observed in the clipped blades. That is, the decline in PSII performance can be considered a measurement artefact rather than an effect caused by the nutrient conditions in the holding tanks.

In their natural environment, and in the holding tanks, the blade's movement constantly changes the seaweed's exposure to light, causing frequent shading and variable blade boundary layer flow conditions. Fixing the blade in a position will remove such variability, creating an environment in which the blade is exposed to direct light and less variable boundary layer flow. While in this experiment, the intensity of the PAR incident at the plane of the fixed blade was measured by the fluorometer (Figs 2 and 6), the blade boundary flow was not quantified. In future experiment, if quantified with suitable measurements, variable and constant light and flow conditions could be used as treatments to study their role in the PSII performance. The wavemakers used in this experiment, for example, could be set to created oscillating flow, and variable light exposure could be generated by switching on/off a series of lights.

PSII response to warming

In Experiment 1, *U. pinnatifida*'s PSII performance appeared to improve after moderate warming (~19 °C) but declined at higher temperatures (~23 °C), with α values rising by ~12 % at 19 °C and falling by ~20–25 % at 23 °C (Table 2, Fig. 8). This pattern is consistent with previous studies of brown macroalgae by Capone et al. (2024) showing enhanced photosynthetic performance under moderate warming but reduced performance near upper thermal limits.

Despite the overall decline in PSII performance throughout the acclimation period of Experiment 2 (Fig. 9), and the warming period in Experiment 3 (Fig. 10), both experiments provided support for the findings of Experiment 1.

In Experiment 2, the notion of a positive effect of moderate warming was supported because the increase in the temperature of the seawater in the Treatment tank from 14 to 18 °C appeared to halt the trend of a decline PSII performance, while the performance of the specimens in the Control tank continued to decline (Table 3, Fig. 9).

In Experiment 3, a gradual temperature increases from 14 to 22 °C caused α to decline in both Control and Treatment tanks, but the decrease was significantly steeper in warming seawater (β = –0.010, t = –3.3, p = 0.001; Table 4, Fig. 10). This statistically confirmed that higher temperature accelerated PSII performance loss, supporting the trend first observed in Experiment 1.

Taken together, these experiments indicate that *U. pinnatifida* may benefit from moderate warming (~18–19 °C) but experiences photo-physiological stress at higher temperatures (~22–23 °C). This pattern is consistent with thermal performance curves described for other kelps, where photosynthetic efficiency peaks at intermediate temperatures and declines near upper thermal limits (Harris et al. 2023). However, due to the limited replication in Experiment 1 (three fluorometers available) and the progressive deterioration of blades in Experiments 2 and 3, the results remain inconclusive with respect to defining the exact thermal tolerance threshold of *U. pinnatifida* PSII. Nonetheless, the consistency of trends across experiments provides meaningful evidence that moderate warming may enhance PSII efficiency, while higher temperatures impose stress.

Future studies in order to address the issue of artefacts, should only mount seaweed blades for the duration of each saturation pulse (SP) analysis. While more labour-intensive, this approach would eliminate the artificial decline associated with long-term clipping and ensure that measured changes in PSII efficiency reflect actual biological responses. Additionally, this would enhance replication potential even with limited PAM fluorometers. Measurements could be made on different blades of the specimen, labelled with tags to track each one. Moreover, instead of performing SP analyses every 30 minutes, investigators could limit measurements to the first hours of the day and adjust the diel light cycle, so pre-light measurements occur during working hours.

Summary and conclusion

This study assessed whether unattended automated PAM fluorometry can reliably measure the PSII photochemical efficiency (α) of *Undaria pinnatifida* under experimental warming. Three laboratory experiments were conducted in which blades were held in fixed positions in front of PAM fluorometers for continuous multi-day monitoring.

Across all experiments, α values consistently declined over time, even under constant temperature, indicating that the measurement setup itself introduced artefacts. The progressive loss of PSII performance suggests that immobilising seaweed blades for extended periods negatively affects photosynthetic efficiency, rather than reflecting a true physiological response to temperature alone.

Despite this limitation, the experiments revealed a consistent trend:

- Experiment 1 indicated enhanced PSII performance at ~19 °C and reduced performance at ~23 °C.
- Experiment 2 qualitatively supported a positive effect of moderate warming (14–18 °C).
- Experiment 3 provided statistical evidence that warming to ~22 °C accelerated the decline in PSII performance compared with the control.

Taken together, these results suggest that *U. pinnatifida* may tolerate or even benefit from moderate warming but experiences stress at higher temperatures. However, due to experimental artefacts and limited replication, the study remains inconclusive regarding the precise thermal response of PSII efficiency.

This work highlights a critical methodological issue: seaweed blades should not remain fixed in position during unattended automated fluorometry. Instead, blades should be mounted only for the duration of individual saturation pulse analyses to avoid confounding effects, ensure tissue health, and enable adequate replication when the number of fluorometers is limited.

By refining PAM fluorometry protocols to eliminate measurement artefacts, future studies will be better equipped to evaluate how seaweeds, including invasive kelps such as *U. pinnatifida*, respond to ocean warming and heatwave conditions.

References

Andersen GS, Pedersen MF, Nielsen SL (2013) Temperature acclimation and heat tolerance of photosynthesis in Norwegian *Saccharina latissima* (Laminariales, Phaeophyceae). *Journal of Phycology* 49(4):689–700.

Barrento S, Camus C, Sousa-Pinto I, Buschmann AH (2016) Germplasm banking of the giant kelp: Our biological insurance in a changing environment. *Algal Research* 13:134–140.

Beer S, Axelsson L (2004) Limitations in the use of PAM fluorometry for measuring photosynthetic rates of macroalgae at high irradiances. *European Journal of Phycology* *39*(1):1–7.

Beer S, Björk M (2000) Measuring rates of photosynthesis of two tropical seagrasses by pulse amplitude modulated (PAM) fluorometry. *Aquatic Botany* *66*(1):69–76.

Bennett S, Wernberg T, De Bettignies T, Campbell AH (2015) Canopy interactions and physical stress gradients in subtidal communities. *Ecology Letters* 18(7):677–686.

Bennett S, Wernberg T, Joy BA, De Bettignies T, Campbell AH (2016) Central and rear-edge populations can be equally vulnerable to warming. *Nature Communications* 7:13925.

Bertness MD, Leonard GH, Levine JM, Schmidt PR, Ingraham AO (1999) Testing the relative contribution of positive and negative interactions in rocky intertidal communities. *Ecology* 80(8):2711–2726.

Bond NA, Cronin MF, Freeland H, Mantua N (2015) Causes and impacts of the 2014 warm anomaly in the NE Pacific. *Geophysical Research Letters* 42(9):3414–3420.

Breitburg D, Levin LA, Oschlies A, Grégoire M, Chavez FP, Conley DJ, Garçon V, Gilbert D, Gutiérrez D, Isensee K, Jacinto GS (2018) Declining oxygen in the global ocean and coastal waters. *Science* 359:1095–9203

Buschbaum C, Chapman AS, Saier B (2006) How an introduced seaweed can affect epibiota diversity in different coastal systems. *Marine Biology* 148:743–754.

Bushinsky SM, Takeshita Y, Williams NL (2019) Observing changes in ocean carbonate chemistry: our autonomous future. *Current Climate Change Reports* 5(3):207–220.

Caputi L, Andreakis N, Mastascusa V, Sordino P, Procaccini G (2016) Temporal correlation of population dynamics and genetic structure in the invasive seaweed *Caulerpa cylindracea*. *Biological Invasions* 18:2139–2154.

Caputi L, Toscano F, Sordino P, Procaccini G (2019) Variability of sexual vs. asexual reproduction and growth traits in the invasive seaweed *Caulerpa cylindracea*. *Marine Environmental Research* 147:45–55.

Carballo JL, Olabarria C, Osuna TG (2002) Analysis of four macroalgal assemblages along the Pacific Mexican coast during and after the 1997–98 El Niño. *Ecosystems* 5(8):749–760.

Capone HE, Brandt M, Gabrielson PW, Bruno JF (2024). Nutrient enrichment can increase the thermal performance of Galápagos seaweeds. *Marine Ecology Progress Series* 749:57–69.

Casado-Amezúa P, Araújo R, Bárbara I, Bermejo R, Borja Á, Díez I, Fernández C, Gorostiaga JM, Guinda X, Hernández I, Juanes JA (2019) Distributional shifts of canopy-forming seaweeds from the Atlantic coast of Southern Europe. *Biodiversity and Conservation* 28(5):1151–1172.

Christensen JH (2007) Regional climate projections. In: S Solomon, D Qin, M Manning, Z Chen, M Marquis, K Averyt et al. (eds) Climate Change (2007): The Physical Science Basis. Contribution of Working Group I to the Fourth Assessment Report of the Intergovernmental Panel on Climate Change. Cambridge: Cambridge University Press.

Davison IR, Pearson GA (1996) Stress tolerance in intertidal seaweeds. *Journal of Phycology* 32(2):197–211.

Deutsch C, Penn JL, Lucey N (2024) Climate, oxygen, and the future of marine biodiversity. *Annual Review of Marine Science* 16(1):217–245.

Egan S, Fernandes ND, Kumar V, Gardiner M, Thomas T (2014) Bacterial pathogens, virulence mechanisms, and host defence in marine macroalgae. *Environmental Microbiology* 16(4):925–938.

Eggert A (2012) Seaweed responses to temperature. In: C Wiencke, K Bischof (eds) Seaweed Biology: Novel Insights into Ecophysiology, Ecology and Utilization. Ecological Studies, vol. 219. Berlin, Heidelberg: Springer, pp.47–66.

Fernández C (2011) The retreat of large brown seaweeds on the north coast of Spain: the case of *Saccorhiza polyschides*. *European Journal of Phycology* 46(4):352–360.

Filbee-Dexter K, Wernberg T (2018) Rise of turfs: a new battlefront for globally declining kelp forests. *Bioscience* 68(2):64–76.

Franco JN, Wernberg T, Bertocci I, Jacinto D, Maranhão P, Pereira T, Martínez B, Arenas F, Sousa-Pinto I, Tuya F (2017) Modulation of different kelp life stages by herbivory: compensatory growth versus population decimation. *Marine Biology* 164(8):1–10.

Franklin LA, Foster RM (1997) The changing irradiance environment: Consequences for marine macrophyte physiology, productivity and ecology. *European Journal of Phycology* 32(3):207–232.

Frölicher TL, Laufkötter C (2018) Emerging risks from marine heat waves. *Nature Communications* 9:650.

Frölicher TL, Fischer EM, Gruber N (2018) Marine heatwaves under global warming. *Nature* 560:360–376.

Gao K, Helbling EW, Häder DP, Hutchins DA (2012) Responses of marine primary producers to interactions between ocean acidification, solar radiation, and warming. *Marine Ecology Progress Series* 470:167–189.

Gaylord B, Rosman JH, Reed DC, Koseff JR, Fram J, MacIntyre S, Arkema K, McDonald C, Brzezinski MA, Largier JL, Monismith SG (2007) Spatial patterns of flow and their modification within and around a giant kelp forest. *Limnology and Oceanography* 52(5):1838–1852.

Genty B, Briantais JM, Baker NR (1989) The relationship between the quantum yield of photosynthetic electron transport and quenching of chlorophyll fluorescence. *Biochimica et Biophysica Acta (BBA)-General Subjects* 990(1):87–92.

Hanelt D, Wiencke C, Karsten U, Nultsch W (1997) Photoinhibition and recovery after high light stress in different developmental and life history stages of *Laminaria saccharina* (Phaeophyta). *Journal of Phycology* 33:387–395.

Haraguchi H, Tanaka K, Imoto Z, Hiraoka M (2009) The decline of *Ecklonia cava* in Kochi, Japan and the challenge in marine afforestation. *Kuroshio Science* 3(1):49–54.

Harris RJ, Bryant C, Coleman MA, Leigh A, Briceño VF, Arnold PA, Nicotra AB (2023) A novel and high-throughput approach to assess photosynthetic thermal tolerance of kelp using chlorophyll α fluorometry. *Journal of Phycology* 9(1):179–192.

Harley CDG, Anderson KM, Demes KW, Jorve JP, Kordas RL, Coyle TA, Graham MH (2012) Effects of climate change on global seaweed communities. *Journal of Phycology* 48(5):1064–1078.

Hobday AJ, Alexander LV, Perkins SE, Smale DA, Straub SC, Oliver EC, Benthuysen JA, Burrows MT, Donat MG, Feng M, Holbrook NJ (2016). A hierarchical approach to defining marine heatwaves. *Progress in Oceanography* 141:227–238.

Hoegh-Guldberg O, Bruno JF (2010) The impact of climate change on the world's marine ecosystems. *Science* 328:1523–1528.

Hoegh-Guldberg O, Poloczanska ES (2017) Editorial: the effect of climate change across ocean regions. *Frontiers in Marine Science* 4:361.

Hoek C van den (1982) Phytogeographic distribution groups of benthic marine algae in the North Atlantic Ocean. A review of experimental evidence from life history studies. *Helgoländer Meeresuntersuchungen* 35(2):153–214.

Holbrook NJ, Scannell HA, Sen Gupta A, Benthuysen JA, Feng M, Oliver ECJ, Alexander LV, Burrows MT, Donat MG, Hobday AJ, Moore PJ, Perkins-Kirkpatrick SE, Smale DA, Straub SC, Wernberg T (2019) A global assessment of marine heatwaves and their drivers. *Nature Communications* 10(1):2624.

Hurd CL, Harrison PJ, Bischof K, Lobban CS (2014). Seaweed ecology and physiology. Cambridge University Press, 17.

IPCC (2021) Climate Change: The Physical Science Basis. Contribution of Working Group I to the Sixth Assessment Report of the Intergovernmental Panel on Climate Change. Cambridge: Cambridge University Press.

Johnson S, Stockdale T, Ferranti L, Balmaseda M, Molteni F, Magnusson L, Tietsche S, Decremer D, Weisheimer A, Balsamo G, Keeley S, Mogensen K, Zuo H, Monge-Sanz B (2019) SEAS5: the new ECMWF seasonal forecast system. *Geoscientific Model Development* 12:1087–1117.

Kitajma MBWL, Butler WL (1975) Quenching of chlorophyll fluorescence and primary photochemistry in chloroplasts by dibromothymoquinone. *Biochimica et Biophysica Acta (BBA)-Bioenergetics* 376(1):105–115.

Klughammer C, Schreiber U (2008) Complementary PS II quantum yields calculated from simple fluorescence parameters measured by PAM fluorometry and the Saturation Pulse method. *PAM Application Notes 1*(2):201–247.

Koch M, Bowes G, Ross C, Zhang X (2013) Climate change and ocean acidification effects on seagrasses and marine macroalgae. *Global Change Biology* 19(1):103–132.

Kordas RL, Harley CD, O'Connor MI (2011) Community ecology in a warming world: the influence of temperature on interspecific interactions in marine systems. *Journal of Experimental Marine Biology and Ecology* 400(1–2):218–226.

Krumhansl KA, Okamoto DK, Rassweiler A, Novak M, Bolton JJ, Cavanaugh KC, Connell SD, Johnson CR, Konar B, Ling SD, Micheli F, Norderhaug KM, Pérez-Matus A, Sousa-Pinto I, Reed DC, Salomon AK, Shears NT, Wernberg T, Anderson RJ, Barrett NS, Buschmann AH, Carr MH, Caselle JE, Derrien-Courtel S, Edgar GJ, Edwards M, Estes JA, Goodwin C, Kenner MC, Kushner DJ, Moy FE, Nunn J, Steneck RS, Vásquez J, Watson J, Witman JD, Byrnes JEK (2016) Global patterns of kelp forest change over the past half-century. *Proceedings of the National Academy of Sciences* 113(48):13785–13790.

Kumar YN, Poong S-W, Gachon C, Brodie J, Sade A, Lim PE (2020) Impact of elevated temperature on the physiological and biochemical responses of *Kappaphycus alvarezii* (Rhodophyta). *PLOS One* 15(9):e0239097.

Le Nohaïc M, Ross CL, Cornwall CE, Comeau S, Lowe R, McCulloch MT, Schoepf V (2017) Marine heatwave causes unprecedented regional mass bleaching of thermally resistant corals in northwestern Australia. *Scientific Reports* 7:1–11.

Li Yuxiao, Hao R, Yu K, Chen X (2024) Short-term impact of decomposing Crown-of-Thorn Starfish blooms on reef-building corals and benthic algae: A laboratory study. *Water* 16(2):190.

Lima FP, Wethey DS (2012) Three decades of high-resolution coastal sea surface temperatures reveal more than warming. *Nature Communications* 3(1):704.

Ling SD, Johnson CR, Ridgway KR, Hobday AJ, Haddon M (2009) Climate-driven range extension of a sea urchin: inferring future trends by analysis of recent population dynamics. *Global Change Biology* 15(3):719–731.

Madin EMP, MacNeil MA, Hill NA, Beger M, Holmes TH, Schaffelke B, Jona-Lasinio G (2012) Socio economic and management implications of range-shifting species in marine systems. *Global Environmental Change* 22(2):137–146.

McCoy SJ, Widdicombe S (2019) Thermal plasticity is independent of environmental history in an intertidal seaweed. *Ecology and Evolution* 9(23):13402–13412.

McNie A, Breen D, Vopel K (2025) Effects of experimental CO_2 enrichment on the PSII photochemical efficiency of *Symbiodinium* sp. in *Acropora millepora*. *Qeios* 7:1–13

Mills KE, Pershing AJ, Brown CJ, Chen Y, Chiang FS, Holland DS, Lehuta S, Nye JA, Sun JC, Thomas AC, Wahle RA (2013) Fisheries management in a changing climate: lessons from the 2012 ocean heat wave in the Northwest Atlantic. *Oceanography* 26(2):191–295.

O'Brien JM, Scheibling RE (2016) Nipped in the bud: mesograzer feeding preference contributes to kelp decline. *Ecology* 97:1873–1886.

Oliver EC, Benthuysen JA, Bindoff NL, Hobday AJ, Holbrook NJ, Mundy CN, Perkins-Kirkpatrick SE (2017) The unprecedented 2015/16 Tasman Sea marine heatwave. *Nature Communications* 8(1):1–12.

Oliver EC, Donat MG, Burrows MT, Moore PJ, Smale DA, Alexander LV, Benthuysen JA, Feng M, Sen Gupta A, Hobday AJ, Holbrook NJ (2018) Longer and more frequent marine heatwaves over the past century. *Nature Communications* 9(1):1324.

Pecl GT, Araújo MB, Bell JD, Blanchard J, Bonebrake TC, Chen IC, Clark TD, Colwell RK, Danielsen F, Evengård B, Falconi L (2017) Biodiversity redistribution under climate change: Impacts on ecosystems and human well-being. *Science* 355(6332):9214.

Reed D, Washburn L, Rassweiler A, Miller R, Bell T, Harrer S (2016) Extreme warming challenges sentinel status of kelp forests as indicators of climate change. *Nature Communications* 7(1):13757.

Roleda MY (2009) Photosynthetic response of Arctic kelp zoospores exposed to radiation and thermal stress. *Photochemical and Photobiological Sciences* 8(9):1302–1312.

Schaeffer A, Roughan M (2017) Subsurface intensification of marine heatwaves off southeastern Australia: the role of stratification and local winds. *Geophysical Research Letters* 44(10):5025–5033.

Schoeman DS, Boyd PW, Cheung WWL, Clarke A, Chen IC, Dupont S, Halpern BS, Hinson A, Howes EL, Lee J, Nielsen EE, O'Brien K, Pörtner HO, Strugnell JM, Sumaila UR, Tunnicliffe V, van Hooidonk R, Warman CG, Richardson AJ (2021) Observed impacts of climate change on marine life. *Nature Climate Change* 11:988–996.

Schreiber U (2004) Pulse-Amplitude-Modulation (PAM) fluorometry and saturation pulse method: an overview. In: Papageorgiou GC, Govindjee (eds) Chlorophyll a Fluorescence. Advances in Photosynthesis and Respiration, vol. 19. Dordrecht: Springer, pp. 279–319.

Smale DA, Wernberg T (2013) Extreme climatic event drives range contraction of a habitat-forming species. *Proceedings of the Royal Society B: Biological Sciences* 280(1754):20122829.

Smale D A, Wernberg T, Oliver E C J, Thomsen M, Harvey B P, Straub SC, Burrows M T, Alexander L V, Benthuysen J A, Donat M G, Feng M, Hobday A J, Holbrook N J, Perkins-Kirkpatrick S E, Scannell H A, Sen Gupta A, Payne B L, Moore PJ (2019) Marine heatwaves threaten global biodiversity and the provision of ecosystem services. *Nature Climate Change* 9(4):306–312.

South PM, Floerl O, Forrest BM, Thomsen MS (2017) A review of three decades of research on the invasive kelp *Undaria pinnatifida* in Australasia: an assessment of its success, impacts and status as one of the world's worst invaders. *Marine Environmental Research* 131:243–257.

Straub SC, Wernberg T, Thomsen MS, Moore PJ, Burrows MT, Harvey BP, Smale DA (2019) Resistance, extinction, and everything in between–The diverse responses of seaweeds to marine heatwaves. *Frontiers in Marine Science* 6:763.

Takahashi S, Murata N (2008) How do environmental stresses accelerate photoinhibition? *Trends in Plant Science* 13(4):178–182.

Terada R, Nakashima Y, Borlongan IA, Shimabukuro H, Kozono J, Endo H, Shimada S, Nishihara GN (2020) Photosynthetic activity including the thermal and chilling light sensitivities of a temperate Japanese brown alga *Sargassum macrocarpum*. *Phycological Research* 68(1):70–79.

Thomsen MS, South PM (2019) Communities and attachment networks associated with primary, secondary and alternative foundation species, a case study of stressed and disturbed stands of Southern Bull Kelp. *Diversity* 11(4):56.

Thomsen MS, Mondardini L, Alestra T, Gerrity S, Tait L, South PM, Lilley SA, Schiel DR (2019) Local extinction of bull kelp (*Durvillaea* spp.) due to a marine heatwave. *Frontiers in Marine Science* 6:501

Tuya F, Cacabelos E, Duarte P, Jacinto D, Castro J, Silva T, Bertocci I, Franco J, Arenas F, Coca J, Wernberg T (2012) Patterns of landscape and assemblage structure along a latitudinal gradient in ocean climate. *Marine Ecology Progress Series* 466:9–19.

Vásquez JAJ, Zuñiga S, Tala F, Piaget N, Rodríguez DC, Vega JMA (2014) Economic valuation of kelp forests in northern Chile: values of goods and services of the ecosystem. *Journal of Applied Phycology* 26:1081–1088.

Wernberg T, Filbee-Dexter K (2019) Missing the marine forest for the trees. *Marine Ecology Progress Series* 612:209–215.

Wernberg T, Straub SC (2016) Impacts and effects of ocean warming on seaweeds. In: Laffoley D, Baxter JM (eds) Explaining ocean warming: Causes, scale, effects and consequences. *IUCN* 87–103

Wernberg T, Bennett S, Babcock RC, De Bettignies T, Cure K, Depczynski M, Dufois F, Fromont J, Fulton CJ, Hovey RK, Harvey ES (2016) Climate-driven regime shift of a temperate marine ecosystem. *Science* 353(6295):169–172.

Wernberg T, Coleman MA, Bennett S, Thomsen MS, Tuya F, Kelaher BP (2018) Genetic diversity and kelp forest vulnerability to climatic stress. *Scientific Reports* 8(1):1851

Wernberg T, Kendrick GA, Phillips JC (2003) Regional differences in kelp-associated algal assemblages on temperate limestone reefs in south-western Australia. *Diversity and Distributions* 9(6):427–441.

Wernberg T, Krumhansl K, Filbee-Dexter K, Pedersen MF (2019) Status and trends for the world's kelp forests. In: Sheppard C (ed) World Seas: An Environmental Evaluation. 2nd ed. Academic Press, pp.57–78.

Wernberg T, Russell BD, Thomsen MS, Gurgel CFD, Bradshaw CJA, Poloczanska ES, Connell SD (2011a) Seaweed communities in retreat from ocean warming. *Current Biology* 21(21):1828–1832.

Wernberg T, Smale DA, Tuya F, Thomsen MS, Langlois TJ, de Bettignies T, Bennett S, Rousseaux CS (2013) An extreme climatic event alters marine ecosystem structure in a global biodiversity hotspot. *Nature Climate Change* 3(1):78–82.

Wernberg T, Russell BD, Moore PJ, Ling SD, Smale DA, Campbell A, Coleman MA, Steinberg PD, Kendrick GA, Connell SD (2011c) Impacts of climate change in a global hotspot for temperate marine biodiversity and ocean warming. *Journal of Experimental Marine Biology and Ecology* 400(1–2):7–16.

Wernberg T, Thomsen MS, Tuya F, Kendrick GA (2011b) Biogenic habitat structure of seaweeds changes along a latitudinal gradient in ocean temperature. *Journal of Experimental Marine Biology and Ecology* 400(1–2):264–271.

Zeebe RE (2012). History of seawater carbonate chemistry, atmospheric CO_2, and ocean acidification. *Annual Review of Earth and Planetary Sciences* 40(1):141–165.

Zhang X, Xu D, Guan Z, Wang S, Zhang Y, Wang W, Zhang X, Fan X, Li F, Ye N (2020) Elevated CO_2 concentrations promote growth and photosynthesis of the brown alga *Saccharina japonica*. *Journal of Applied Phycology* 32(3):1949–1959.